

RSC Advances



This is an *Accepted Manuscript*, which has been through the Royal Society of Chemistry peer review process and has been accepted for publication.

Accepted Manuscripts are published online shortly after acceptance, before technical editing, formatting and proof reading. Using this free service, authors can make their results available to the community, in citable form, before we publish the edited article. This *Accepted Manuscript* will be replaced by the edited, formatted and paginated article as soon as this is available.

You can find more information about *Accepted Manuscripts* in the [Information for Authors](#).

Please note that technical editing may introduce minor changes to the text and/or graphics, which may alter content. The journal's standard [Terms & Conditions](#) and the [Ethical guidelines](#) still apply. In no event shall the Royal Society of Chemistry be held responsible for any errors or omissions in this *Accepted Manuscript* or any consequences arising from the use of any information it contains.

Punica granatum (pomegranate) peel extract exerts potent antitumor and anti-metastasis activity in thyroid cancer

Yujue Li,^{†a} Tinghong Ye,^{†b} Fangfang Yang,^{†b} Mingxing Hu,^b Libo Liang,^a He He,^c Zhipeng Li,^a Anqi Zeng,^b Yali Li,^b Yuqin Yao,^b Yongmei Xie,^b Zhenmei An^{*a} and Shuangqing Li^{a*}.

^a Department of Endocrinology and Metabolism, Department of General Practice Medicine, West China Hospital, Sichuan University, Chengdu, China

^b State Key Laboratory of Biotherapy and Department of Liver Surgery, West China Hospital, Sichuan University and Collaborative Innovation Center for Biotherapy, Chengdu, China

^c Department of Laboratory Medicine, West China Hospital, Sichuan University, Chengdu, China

[†] These authors contributed equally to this work.

*Corresponding author: lsqhxjk@126.com (Shuangqing Li), anzm1997@sina.com (Zhenmei An), Tel.: +86 28 85503817, Fax: +86 28 85164060.

Abstract

The incidence of thyroid carcinoma is obviously rising throughout the world in past ten years. However, over treatment usually occurred in thyroid carcinoma without new and effective approach explored. In this study, punica granatum (pomegranate) peel extract (PoPx), a kind of herb, was evaluated for its anticancer activity to thyroid carcinoma *in vitro* and *in vivo*. PoPx potently suppressed proliferation in two kinds of thyroid cancer cell lines, and induced cancer cells apoptosis. Besides, PoPx could also decrease the mitochondrial membrane potential ($\Delta\Psi_m$), indicating that PoPx may induce apoptosis *via* mitochondria-mediated apoptotic pathway. In addition, PoPx markedly impaired thyroid cancer cell migration and invasion by down-regulating

expression of matrix metalloproteinase-9 (MMP-9). More importantly, PoPx significantly inhibited tumor growth in the BCPAP-bearing mice model by reducing cell proliferation and inducing apoptosis. These findings suggested that PoPx could be an effective phytochemical agent.

Introduction

As one of the most common endocrine malignancy, the increasing incidence of thyroid cancer in the world has drawn public attention.¹ About 95% thyroid cancer derive from the thyroid follicular epithelial cells, including papillary thyroid carcinoma (PTC, 80%), follicular thyroid carcinoma (FTC, 10%-15%), poorly differentiated thyroid cancer (PDTC) and anaplastic thyroid cancer (ATC, 1%-2%).³ The survival rate of thyroid cancer is relatively higher than any other malignant tumors, especially PTC. However, the recurrence and mortality is still a challenge for thyroid cancer treatment. Traditional treatment of thyroid cancer includes surgical resection, postoperative radio therapy, thyroid stimulating hormone (TSH) suppression treatment and small molecule multi-targeted kinase inhibitors (MKI) emerging as a new choice for thyroid cancer.⁴ As the major treatment of thyroid cancer, surgery affects the patient's quality of life with many postoperative complications. Postoperative radioactive iodine treatment can destroy residual thyroid tumor or distant metastasis and obliterate the residual thyroid tumor tissue, but its curative effect depends on the uptake rate of I^{131} , which limits its application. It's beneficial for patients to keep low-level of TSH after surgery to reduce cancer recurrence and prolong life, but subclinical hyperthyroidism caused by long-term TSH suppression also has side-effect on cardiovascular system, skeletal system and other aspects.^{5,6} However, efficacy and safety of targeted drugs remain to be confirmed by further research. Therefore, it is necessary to find a new way to prevent and treat thyroid cancer.⁷

Traditional Chinese Medicine (TCM) has precious value in disease prevention and health care.⁸⁻¹² In recent years, the pomegranate as a natural medicine and health food is widely used all over the world. Continuous research about the bioactivity of

pomegranate has gradually drawn the attention of scholars.¹³⁻¹⁵ It was reported that pomegranate peel extract (PoPx) has various bioactivities in regulating blood glucose level,¹⁶ oxidation resistance,¹⁷ anti-bacteria,¹⁸ etc.^{19,20} Recently, some studies have showed that PoPx inhibits tumor growth of prostate cancer,²¹ colon cancer,²² skin cancer²³ and breast cancer²⁴ by inducing cell apoptosis.

However, the effect of PoPx on thyroid cancer has not been reported yet, and further research is needed to illustrate the mechanism of PoPx. To provide evidence for wide application of PoPx in thyroid cancer prevention and treatment, the effect of PoPx was assessed on BCPAP and TPC-1 papillary thyroid carcinoma cells and the preliminary molecular mechanism was explored in our study.

Materials and methods

Preparation of PoPx

The pomegranate peels of Tunisia soft-seed pomegranate were obtained from Yuzhuang Ecological Green Industry Co. (Qianxi County, Guizhou Province, China). The preparation of pomegranate peel extract referred to previously described methods with minor modification.²⁵ The fresh peels (400g) were cut into pieces in size of 0.5cm and extracted with the combination of ethanol (1550mL) and H₂O (480mL), following soaked for 2h at 60°C, then crude extracts were filtered and concentrated under vacuum, 45g brown powder solid was collected at last. PoPx was stored in -20°C protected from light before use.

Reagents and antibodies

3-(4,5-Dimethylthiazol-2-yl)-2,5-diphenyltetrazoliumbromide (MTT), dimethyl sulfoxide (DMSO), 2-(6-Amino-3-imino-3H-xanthen-9-yl)benzoic acid methyl ester (Rh123) and 2',7'-dichlorodihydrofluorescein diacetate (DCFH-DA) were purchased from Sigma Chemical Co. (St Louis, MO, U.S.A.). Hoechst 33258 was purchased from Beyotime (Beijing, China). The Annexin V-FITC Apoptosis Detection Kit was purchased from KeyGen Biotech (Nanjing, China). For western blot experiments, the primary antibodies against matrix metalloproteinase-9 (MMP-9), Bax and β -actin

were purchased from Cell Signaling Technology (Beverly, MA, U.S.A.) and secondary antibodies were from ZSGB-BIO Co. (Beijing, China). For immunohistochemistry studies, the primary antibodies against cleaved caspase-3 (CC-3) and matrix metalloproteinase-9 (MMP-9) were purchased from Cell Signaling Technology (Beverly, MA, U.S.A.). Mouse monoclonal anti Ki-67 was purchased from Merck-Millipore. DAB Detection Kit was from ZSGB-BIO Co. (Beijing, China).

For *in vitro* assays, PoPx was prepared as 200mg/mL stock solution in DMSO and stored at -20°C. Then the stock solution diluted in the relevant assay medium, and 0.1% DMSO served as a vehicle control. For *in vivo* studies, PoPx was dissolved in normal saline and dosed at 125mg/kg and 62.5mg/kg of body weight.

High performance liquid chromatography (HPLC) and mass spectrography (MS)

Waters 2695 HPLC system (Waters Corp., Milford, Massachusetts, U.S.A.) was used in this experiment. The method and chromatographic condition referred to previously described methods.²⁶ Data were processed by Waters Empower 3 software. The chromatographic separation was conducted on Waters Symmetry C18 column (5µm, 4.6×250mm). The mobile phase consisted of deionized water with glacial acetic acid (A; 99:1, v/v; pH 3.0) and methanol (B) with a flow rate of 1mL/min. The gradient program was set as follows: 0-70min, 10-45%B; 70-80min, 45%B. The chromatogram was detected at wave length of 256nm throughout the assay. Absciex Qtrap 5500 was used in MS. We detected the samples by HPLC and MS after establishing the standard working curves of ellagic acid (EA) and punicalagin (PC).

Cell culture

The human papillary thyroid cancer cell lines BCPAP (harboring BRAF V600E mutation) was obtained from University of Medicine Lyon-Sud and TPC-1 (harboring RET-PTC rearrangement) from Institute of Interdisciplinary Research. Nthy-ori 3-1 (human thyroid follicular epithelial cell line) was obtained from Health Protection

Agency Culture Collection. All the other human normal cell lines used in our study were obtained from the American Type Culture Collection. Cells were propagated in RPMI 1640 or DMEM medium containing 10% heat-inactivated fetal bovine serum (FBS) and 1% antibiotics (penicillin and streptomycin) in 5% CO₂ at 37°C.

Cell viability assay

The cell viability of PoPx-treated thyroid cancer cells was assessed by MTT assay. Briefly, the exponentially growing cells ($2-6 \times 10^3$ cells/well) were plated in 96-well plates (100 µL/well) and incubated for 24h. Then the cells were treated with different concentrations of PoPx (0, 12.5, 25, 50, 100, 200 µg/mL). After treatment for 24h, 48h and 72h, respectively, the 20 µL of 5mg/ml MTT was added to each well, and the plates were incubated at 37°C for additional 2-4h. The medium was subsequently removed, the purple colored precipitates of formazan were dissolved in 150 µL of DMSO. The color absorbance was recorded at 492nm using a Spectra MAX M5 microplate spectrophotometer (Molecular Devices, CA, U.S.A.). In addition, the 72h MTT assay was conducted on HEK293 (human embryonic kidney cell line) and LO2 (human normal liver cell line). Meanwhile, 24h, 48h and 72h MTT assay was also operated on Nthy-ori 3-1 (human thyroid follicular epithelial cell line) to test the cytotoxicity of PoPx. Data shown represents the average of three independent experiments.

Colony formation assay

Colony formation assay was measured as previously described.²⁷ Briefly, BCPAP and TPC-1 cells were seeded with specified number (2000 cells/well) in 6-well plates. After 24h incubation, the cells were treated with designed concentrations of PoPx (0, 12.5, 25, 50, 100, 200 µg/mL) and then incubated for additional 10 days. Then the cells were fixed with methanol and stained with a 0.5% crystal violet solution about 15 minutes and the colonies (>50 cells) were counted under microscope. Data shown represents the average of three independent experiments.

Morphological analysis of nuclei by Hoechst staining

An apoptotic cell has distinct morphologic characteristics: cell body shrinkage, chromatin condensation and margination as well as emerging apoptotic bodies.²⁸ To identify whether the PoPx-inducing reduction in cell proliferation was attributable to apoptosis, we stained the BCPAP and TPC-1 cells with Hoechst 33258 dye. In brief, BCPAP and TPC-1 cells ($1-2 \times 10^5$ cells/well) were plated onto 18-mm coverglass in a 6-well plate for 24h respectively. After treatment with different concentrations (0, 12.5, 25, 50, 100, 200 $\mu\text{g}/\text{mL}$) of PoPx for following 48h, the cells were washed with ice-cold phosphate-buffered saline (PBS) twice and fixed in methanol for 15 minutes. The cells were stained with the Hoechst 33258 solutions in accordance with the manufacturer's instruction. Then nuclear morphology of apoptotic cells was photographed under a fluorescence microscopy (Leica, DM4000B).

Apoptosis analysis by Flow Cytometry (FCM)

To further confirm the apoptosis inducing by PoPx, AnnexinV-FITC apoptosis detection kit was used as described before.²⁹ In short, cells ($1-2 \times 10^5$ cells/well) were seeded in 6-well plates and treated with PoPx (0, 12.5, 25, 50, 100, 200 $\mu\text{g}/\text{mL}$) for 48h. Then the cells were harvested and washed twice with cold PBS. The level of apoptosis was detected using the apoptosis detection kit referring to manufacturer's instruction by FCM. The data were analyzed with FlowJo software. Data shown represents the average of three independent experiments.

Detection of mitochondrial membrane potential (Ψ_m) and reactive oxygen species (ROS)

Mitochondrial membrane potential assay was performed as previously reports, examined by FCM using Rh123 staining.³⁰ Cells were treated with indicated doses of PoPx (0, 12.5, 25, 50, 100, 200 $\mu\text{g}/\text{mL}$) for 48h and then incubated with 10 μM Rh123 at 37 $^\circ\text{C}$ in the dark for approximately 30min. The stained cells were then washed with cold PBS twice, and next Rh123 fluorescence was detected by FCM. For the intracellular ROS detection,³¹ cells were treated with purposed concentrations of PoPx

(0, 12.5, 25, 50, 100, 200 μ g/mL) for 48h and then incubated with 10 μ M DCFH-DA diluted in PBS at 37 $^{\circ}$ C for 30min. The stained cells were then washed with cold PBS and analyzed by FCM. Data shown represents the average of three independent experiments.

Boyden chamber migration and invasion assay

Boyden chamber (8 μ m pore size) migration assay was conducted as previously described, with a few modifications.³² Briefly, a total of 1.5×10^5 cells (for BCPAP) or 1×10^5 cells (for TPC-1) in 100 μ L serum-free medium were added into the top chamber of 24-well transwell plates (Millipore), and 600 μ L medium containing 10% FBS was added at the bottom. Different concentrations of PoPx (0, 25, 100, 200 μ g/mL) were added in both chambers. Cells were allowed to migrate for approximately 48h and non-migrated cells in the top chamber were discarded. Then the migrated cells adhering to the lower surface of the transwell membrane were fixed in methanol and stained with 0.5% crystal violet. Migrated cells in 3 fields selected randomly were counted and photographed under a light microscope. Invasion assay was determined according to previous studies.³³ In brief, the upper surface of the transwell membrane was covered with Matrigel (1:3, 60 μ L/well, BD Biosciences, U.S.A.) diluted by serum-free medium and the lower compartment of the chamber was filled with 600 μ L medium containing 10% FBS. 1.5×10^5 cells (for BCPAP) or 1×10^5 cells (for TPC-1) in 100 μ L serum-free medium were placed in the upper part of each transwell and treated with designed concentrations of PoPx (0, 25, 100, 200 μ g/mL). After incubation for 48h, cells located on the upper side of the filter were removed and the underside were fixed with methanol and stained with 0.5% crystal violet. Then, similarly, migrated cells were counted and photographed under a light microscope. The results were expressed as the percentage inhibition rate of migration compared with vehicle group.

Western blot analysis

To determine the effect of PoPx on involved signaling pathway, some proteins in

BCPAP cells were evaluated by western blot. The western blot analysis was performed as described previously,³⁴ with minor modification. Briefly, BCPAP cells were treated with PoPx in different concentrations (0, 25, 100, 200 μ g/mL) for 48h, then cells were washed twice with cold PBS and lysed in RIPA buffer. After the cell lysates centrifuging at 13300rpm at 4 $^{\circ}$ C for 15min, the supernatant was harvested. The extractive protein concentrations were measured using the Coomassie brilliant blue G-250 method and equalized before loading. Equal amount of protein from each sample was subjected to sodium dodecyl sulfate-polyacrylamid egel electrophoresis (SDS-PAGE) gels and following transferred onto polyvinylidene difluoride (PVDF) membranes (Amersham Bioscience, Piscataway, N.J.). Then, the membranes were blocked with 5% skim milk at 37 $^{\circ}$ C for 2h and incubated with peculiar primary antibodies overnight at 4 $^{\circ}$ C. After incubation with the relevant secondary antibodies, the reactive bands were identified using an enhanced chemiluminescence kit (Amersham Bioscience, Piscataway, N.J.).

Xenograft tumor assay in nude mice

All animal experiments have been approved by the Institutional Animal Care and Treatment Committee of Sichuan University in China (Permit Number: 20151109-2) and were carried out in accordance with the approved guidelines. Female BALB/c nude mice (5-6 weeks old) were obtained from Sichuan University Laboratory Animal Center (Chengdu, China). After the female BALB/c athymic mice adapting to the environment for a week, they were randomized into three groups (8 mice per group), and received intragastric administration (i.g.) of PoPx 125mg/kg, 62.5mg/kg or vehicle, respectively once daily for 6 days. Then we inoculated the mice with BCPAP cell (2.0×10^6 cells/120 μ L/each). After subcutaneous ectopic cell implantation, treatment discontinued for 7 days and then continued for 18 days. Tumor volume and body weight were measured every three days. The tumor size was calculated according to the formula: Tumor volume (mm^3) = $0.52 \times L \times W^2$ where L is the length and W is the width. At the end of the experiment (on the 31th day), all animals were euthanized by cervical dislocation. Tumors and internal organs, such as, hearts, livers,

spleens, lungs and kidneys were excised from animals.

These tissues (tumors and internal organs) of the mice were fixed in formalin, embedded in paraffin, cut to 4 μ m sections, dried, and kept at room temperature. Immunohistochemistry (IHC) staining was described previously.³⁵ Tumor sections were conducted antigen retrieval, blocked with serum, incubated with primary antibodies (CC-3, Ki-67 and MMP-9), then stained with the DAB Detection Kit. Moreover, to evaluate the effect of PoPx on visceral organs damage of animals, we performed hematoxylin and eosin (H&E) staining of tissue sections (heart, liver, spleen, lung and kidney). Images were taken with Leica microscope (Leica, DM4000B).

Statistical analysis

Cell culture-based experiments were done at least in biological triplicates. Quantifications of staining were done on sections of at least three different views. Data were represented as means \pm SD. The 2-tailed Student's *t* test was used for statistical analysis and statistically significant *p* values were labeled as follows: **p*<0.05; ** *p*<0.01; *** *p*<0.001.

Results

The content and molecular weight of punicalagin and ellagic acid in PoPx

Linear regression analysis for punicalagin (PC) and ellagic acid (EA) was expressed by plotting the peak area (*y*) against the concentrations (*x*, μ g/mL) of standard solutions, as shown in Table 1. All the analytes presented high linearity in the investigated ranges. The sample of PoPx was analyzed using the optimized HPLC method and matched by *the Similarity Evaluation System for Chromatographic Fingerprint of Traditional Chinese Medicine* (Version 2012A). Components were identified as PC (peak 1 and peak 2) and EA (peak 3) by comparing with the retention time of standard substances, which was shown in Fig.1A, and chemical structure was shown in Fig.1B. As shown in Fig.1C, the molecular weight of EA (ellagic acid [M-H]⁻: 301.3) and PC (punicalagin [M-H]⁻: 1083.2) was detected by mass spectrum.

The content of PC and EA in PoPx were calculated according to the regression equation and the relevant peak area of PoPx. The results of the analysis reveal that PC accounts for 47.98mg/g and EA accounts for 0.75mg/g in PoPx.

PoPx inhibits proliferation and influences the morphology of thyroid cancer cells

To evaluate the effect of PoPx on thyroid cancer, BCPAP and TPC-1 cell lines were used in this study. As shown in Fig.2B, we investigated the time- and concentration-dependent effect of PoPx on thyroid cancer cells by exposing cells to various concentrations of PoPx (0, 12.5, 25, 50, 100 and 200 μ g/mL) for 24h, 48h and 72h. TPC-1 proliferation increased with 12.5-50 μ g/mL PoPx treatment for 24h. However, 100-200 μ g/mL PoPx treatment inhibited proliferation of TPC-1 obviously. Meanwhile, cell viability decreased with 25-200 μ g/mL PoPx treatment for 48h and 12.5-200 μ g/mL PoPx treatment for 72h. Moreover, low concentrations of PoPx treatment for 24h also did not inhibit the proliferation of BCPAP and only in the concentration 200 μ g/mL of PoPx distinctly reduced proliferation. Furthermore, cell viability decreased with 50-200 μ g/mL PoPx treatment for 48h and 12.5-200 μ g/mL PoPx treatment for 72h in BCPAP. Therefore, we deduced that anti-tumor effect of PoPx is not stable at lower doses in 24 hours. Concentration and drug treating time both affect the effectiveness of anti-proliferation in thyroid cancer cells. After treatment with PoPx for 48h and 72h, respectively, the proliferation of both BCPAP and TPC-1 cell lines were decreased obviously with an IC₅₀ values lessened from 110.8 μ g/mL to 76.9 μ g/mL for BCPAP and from 120.8 μ g/mL to 68.4 μ g/mL for TPC-1. Moreover, we examined the inhibitory effect of PoPx on three normal cell lines (Nthy-ori 3-1, HEK293 and LO2), while the IC₅₀ values were more than 400 μ g/mL (Table 2). In addition, morphology changed of thyroid cancer cells was observed after 48h treatment with PoPx (Fig.2A).

To further investigate whether PoPx could inhibit the proliferation of thyroid cancer cells, we operated colony formation assay after PoPx treatment. Figure 2C clearly showed that clone formation of BCPAP and TPC-1 cells were reduced in a concentration-dependent manner after being exposed to PoPx. Moreover, the number

of the colonies treated with PoPx significantly reduced comparing with control. Taken together, these results implied that PoPx has strong cytostatic and cytotoxic effect on thyroid cancer cells.

PoPx induced cell apoptosis in BCPAP and TPC-1 cell lines

We next explored whether PoPx induced thyroid cancer cells apoptosis. Hoechst 33258 staining assay showed that PoPx treatment resulted in cell shrinking, nuclear fragmentation and formation of condensed nuclei with bright-blue fluoresce. Besides, these changes were concentration-dependent (Fig.3A). The morphologic changes were also observed in TPC-1 cells (Fig.3A).

To further confirm the induction of apoptosis in BCPAP and TPC-1 cells with PoPx treatment, we also investigated the levels of apoptosis using the Annexin V-FITC/PI dual-labeling technique by flow cytometry (FCM). As shown Fig.3B and C, PoPx induced BCPAP cell apoptosis in a concentration-dependent manner. After 48h, the percentage of apoptotic cells (the early apoptotic cells plus the late apoptotic cells) increased from 3.49% to 38.8% as the concentration increased from 0 to 200 μ g/mL, indicating a nearly change of 35.3%. Similar results were observed in TPC-1 cells and the percentages of apoptotic cells at different concentrations are as follows: vehicle (10.09%), 12.5 μ g/mL (8.21%), 25 μ g/mL (12.68%), 50 μ g/mL (20.29%), 100 μ g/mL (37.00%) and 200 μ g/mL (70.50%). Besides, western blotting also confirmed the characterization of PoPx-induced apoptosis. We examined Bax expression levels in BCPAP cells after PoPx-treated for 48h. As shown in Fig.3D, the expression of Bax (a kind of pro-apoptotic protein) increased in a concentration-dependent manner, suggesting that PoPx could induce the apoptosis of thyroid cancer cells.

PoPx induced loss of mitochondrial transmembrane potential ($\Delta\Psi_m$) and ROS generation

In the previous data, the increased level of Bax was observed after treatment with PoPx (Fig.3D). We speculated that PoPx-induced apoptosis might be *via* the

mitochondrial apoptotic pathway. In order to verify the hypothesis, we tested the changes in the mitochondrial membrane potential ($\Delta\Psi_m$) by FCM using a green fluorochrome Rh123. As shown in Fig.4A, B and C, PoPx treatment led the loss of $\Delta\Psi_m$ in BCPAP and TPC-1 cells. Especially in the dose 200 $\mu\text{g}/\text{mL}$, the loss of $\Delta\Psi_m$ in BCPAP increased significantly 56.13% compared with vehicle group after exposure to PoPx for 48h. Similar results were observed in TPC-1 cells. These results suggested that the mitochondria-mediated pathway may be involved in PoPx-induced apoptosis.

Many researches showed that mitochondria play central roles in cellular metabolism and apoptosis and are a major source of reactive oxygen species (ROS).^{36,37} Excessive ROS induces mitochondrial permeability transition (PT) pore opening and cytochrome *c* releasing from mitochondria, which results in $\Delta\Psi_m$ drop, apoptosome formation and caspase activation.³⁸ In order to test the levels of ROS, we stained the cells with DCFH-DA reagent and estimated ROS accumulation by FCM. The results showed that the levels of ROS increased in a dose-dependent manner. The fold changes of ROS level were increased up to 2.1 times in BCPAP cells and to 4.0 times in TPC-1 cells when administrating 200 $\mu\text{g}/\text{mL}$ PoPx (Fig.4D, E and F). These results confirmed that the inhibition of thyroid cancer cells by PoPx is mediated by the induction of apoptosis *via* the mitochondria-mediated apoptotic pathway.

PoPx inhibits thyroid cancer cell migration and invasion

We performed transwell migration assay using BCPAP and TPC-1 cell lines. As shown in Fig.5A, PoPx inhibits migration of both BCPAP and TPC-1 cells in dose-dependent manners. Then, we performed a Matrigel invasion assay. The invasion ability of both BCPAP and TPC-1 cells significantly decreased in the presence of PoPx than vehicle, which could be observed in Fig. 5B explicitly.

Furthermore, considering the relationship between matrix metalloproteinase-9 (MMP-9) and cell migration and invasion, we investigated whether MMP-9 is involved in inhibitory effect on migration and invasion of PoPx. As Fig.3D indicates, PoPx treatment decreased the expression of MMP-9 in BCPAP cells. Taken together, all of these results implied that PoPx inhibited the migration and invasion of thyroid

cancer cells.

Antitumor efficacy of PoPx in xenograft model of human thyroid cancer BCPAP

To determine whether the antitumor activity of PoPx *in vivo* is consistent with its effect *in vitro*, BCPAP tumor-bearing mice were dosed daily at the dose of 62.5mg/kg and 125mg/kg for altogether 24 days before and after inoculation. As shown in Fig.6C, tumor volumes were significantly lower in PoPx-treated mice as compared to control mice. However, as an indicator of health, body weight did not show a significant difference between these three groups throughout the experiments (Fig.6D). At the end of experiments, the tumors were isolated and weighted (Fig.6A and B). As shown in Fig.6B, the mean tumor weight was significantly less in PoPx-treated mice as compared with control mice. To verify the underlying mechanism of PoPx activity, BCPAP-induced tumors collected on day 31 were examined for proliferation and apoptosis. As shown in Fig.6E and F, PoPx significantly increased CC-3-positive cells and decreased Ki-67-positive cells. In addition, there is an increasing evidence to indicate that MMPs have vital roles in tumor invasion and metastasis.³⁹ We also found that treatment with PoPx could inhibit the expression of MMP-9 in BCPAP tumor tissues (Fig.6G). Overall, these data suggest that PoPx suppress thyroid tumor by inhibiting cell proliferation, inducing apoptosis, and blocking metastasis, which is consistent with the *in vitro* data. More importantly, no pathologic changes after PoPx treatment were observed in heart, liver, spleen, lung and kidney by H&E staining (Fig.7), implicating that it may be a safe and effective agent for thyroid cancer therapy at least in xenograft tumor models.

Discussion

The incidence of thyroid cancer is increasing worldwide rapidly in recent years and the prevalence among women is about three times as men especially aged 25-65.² Although thyroid cancer shows relatively good prognosis, cervical lymph node metastasis and aggressive subset are highly associated with the risk of recurrence or death.⁵ In addition, as the major treatment of thyroid cancer, surgery inevitably affects

the patient's quality of life and it also requires strictly indications and contraindications.⁶ Therefore, the development of new clinical approaches for the treatment of thyroid cancer is essential.

Herbal plants have universally been the basis for almost all medicinal therapies throughout human history.^{8,9} Plant extracts have drawn great attention in fields of pharmaceuticals and food since the late 19th century. Recently, natural extracts used in anti-cancer studies have been reported continually: potato extracts kill cancer stem cell,⁴⁰ magnolia extracts hold anti-cancer effect,⁴¹ cinnamon extracts suppress cancer cell growth,⁴² rose hip extracts treat triple-negative breast cancer (ER-, PR-, and HER2-).⁴³ On account of its safety and nutrition, phytochemical would be a promising strategy to provide a supplementary approach for cancer prevention and treatment. Currently, there are lots of researches on different parts of pomegranate have been reported which are known for containing enormous antioxidant and anticancer activity.^{19,20} Our study, therefore, focused on the anticancer effects on thyroid cancer of the extract of pomegranate's peel (PoPx).

In this study, PoPx, a kind of herb extracts, was evaluated for its potency against thyroid cancer *in vitro* and *in vivo*. We firstly detected the content of PC and EA in PoPx, which were 47.98mg/g and 0.75mg/g. These polyphenols constituted the main composition of the extract and played a crucial role in anticancer activity.^{44,45} The MTT assay results showed that PoPx decreased the viability of thyroid cancer cells, and colony formation assay data indicate PoPx inhibited the proliferation of thyroid cancer cells in a time- and dose-dependent manner. Moreover, classic apoptotic morphologic changes were observed in drug-treated cells, including reduction of cell volume and formation of a circular morpholog , these not seen in control group cells.

Apoptosis, a cell suicide program, maintains tissue homeostasis and eliminates unwanted or damaged cells from multicellular organisms, which is fundamental for the development.⁴⁶ Recently, with the in-depth studies of cell apoptosis, scientists have realized that apoptosis is a key mechanism in tumor cell death.⁴⁷ Hoechst 33258 staining and FCM assays both revealed that PoPx treatment induced apoptosis of thyroid cancer cells in a concentration-dependent manner. There are mainly two kinds

of apoptosis pathways, including the cell death receptor-mediated extrinsic pathway and the mitochondrial-mediated intrinsic pathway. The Bcl-2 family pro-apoptotic protein Bax is involved in the induction of intrinsic apoptosis.⁴⁸ In our study, Bax was upregulated. Furthermore, we found that PoPx significantly increased ROS production in BCPAP and TPC-1 cells. That was consistent with our result of the dose-dependent decrease in the mitochondria membrane potential. In this regard, PoPx may activate some other signaling pathway results in apoptosis. This warrants further investigation. Therefore, in partly, these data indicated that PoPx treatment induced apoptosis in thyroid cancer might be through ROS-mediated mitochondrial apoptotic pathway.

Since not all compounds have potent antitumor activity *in vitro* could exhibit anticancer activity *in vivo*, we examined the antitumor effects of PoPx in our established BCPAP tumor model in BALB/c athymic mice. The results showed that tumor growth was significantly inhibited by PoPx administration (125mg/kg/d) with an inhibitory rate by 69.8%. Meanwhile, increased expression of CC-3 and reduced expression of Ki-67 in tumor tissue were observed after PoPx treatment compared with the untreated groups.

Thyroid cancer starts as a local disease, but it can also metastasize to the lymph node, lung and other organs.⁵⁰ The metastatic process is complex, tumor cells need to enter into blood or lymph vessels as well as extravasate into the secondary organs. Therefore, tumor cell migration and invasion is a vital step in successful cancer metastasis, so inhibiting this step is a practical approach to anti-metastasis treatment. It has been reported that focal adhesion kinase (FAK)/MMP-involved pathway is critical to cancer invasion and metastasis.⁵¹ MMP-9 up-regulation can significantly enhance tumor cell metastatic potential in thyroid cancer.⁵² In this study, PoPx down-regulated MMP-9 expression in BCPAP cells and tumor tissues. The results suggested PoPx may inhibit thyroid cancer metastasis by blocking MMPs signaling pathway.

In summary, our study provided important information regarding the antitumor activities of punica granatum (pomegranate) peel extract (PoPx) in thyroid cancer and showed that PoPx inhibits thyroid cancer cell proliferation, migration and invasion,

and induces cell apoptosis through the mitochondria-mediated intrinsic pathway. Furthermore, PoPx may have particularly high potential for thyroid cancer treatment, as supported by its profound inhibitory effect on the growth of xenograft thyroid tumors without significant visceral organ injury. In addition, the PoPx is easy to achieve. Although this is the first study to demonstrate the antitumor effect of PoPx in thyroid cancer, the compelling evidence indicated that PoPx might be a potential candidate for blocking thyroid cancer growth and metastasis.

Acknowledgement

The authors would like to thank Chen Fan for her technical assistance. This study was funded by the grants from the National Natural Science Foundation of China (81500054 and 81402564), China Postdoctoral Science Foundation (2015M570788 and 2016T90859), Technology Department of Sichuan Province (2014SZ0170 and 2015SZ0174).

References

- 1 B. A. Kilfoy, T. Zheng, T. R. Holford, X. Han, M. H. Ward, A. Sjodin, Y. Zhang, Y. Bai, C. Zhu, G. L. Guo, N. Rothman and Y. Zhang, *Cancer Causes Control*, 2009, 20, 525-531.
- 2 P. Nix, A. Nicolaides and A. P. Coatesworth, *Int. J. Clin. Pract.*, 2005, 59, 1340-1344.
- 3 S. K. G. Grebe, *Expert Rev. Endocrinol Metab.*, 2009, 4, 25-43.
- 4 P. Perros, K. Boelaert, S. Colley, C. Evans, R. M. Evans, G. G. Ba, J. Gilbert, B. Harrison, S. J. Johnson and T. E. Giles, *Clin. Endocrinol.*, 2014, 81(S1), 1-122.
- 5 S. Yamashita, N. Amino and Y. K. Shong, *Thyroid*, 2011, 21, 577-580.
- 6 S. J. Mandel and L. Mandel, *Thyroid*, 2003, 13, 265-271.
- 7 R. M. Carneiro, B. A. Carneiro, M. Agulnik, P. A. Kopp and F. J. Giles, *Cancer Treat Rev.*, 2015, 41, 690-698.
- 8 J. M. Luk, X. Wang, P. Liu, K. F. Wong, K. L. Chan, Y. Tong, C. K. Hui, G. K. Lau and S. T. Fan, *Liver Int.*, 2007, 27, 879-890.
- 9 Y. Chen, J. Zhu and W. Zhang, *Anticancer Drugs*, 2014, 25, 983-991.
- 10 T. S. Cheung, T. H. Song, T. B. Ng, F. H. Wu, L. X. Lao, S. C. Tang, J. C. Ho, K. Y. Zhang and S. C. Sze, *Curr. Med. Chem.*, 2015, 22, 2392-2403.
- 11 G. D. Sun, C. Y. Li, W. P. Cui, Q. Y. Guo, C. Q. Dong, H. B. Zou, S. J. Liu, W. P. Dong and L. N. Miao, *J. Diabetes Res.*, 2016, 5749857.

- 12 A. Wang, L. Lin and Y. Wang, *Am. J. Chin. Med.*, 2015, 43, 601-620.
- 13 S. T. Lee, M. H. Lu, L. H. Chien, T. F. Wu, L. C. Huang and G. I. Liao, *BMC Complem. Altern. Med.*, 2013, 13, 2049-2057.
- 14 S. M. Finegold, P. H. Summanen, K. Corbett, J. Downes, S. M. Henning and Z. Li, *Nutrition*, 2014, 30, 1210-1212.
- 15 F. Les, J. M. Prieto, J. M. Arbonesmainar, M. S. Valero and V. Lopez, *Food Funct.*, 2015, 6, 2049-2057.
- 16 S. Akhtar, T. Ismail, D. Fraternali and P. Sestili, *Food Chem.*, 2015, 174, 417-425.
- 17 G. Yuan, H. Lv, B. Yang, X. Chen and H. Sun, *Molecules*, 2015, 20, 11034-11045.
- 18 S. R. Foss, C. V. Nakamura, T. Uedanakamura, D. A. Cortez, E. H. Endo and B. P. D. Filho, *Ann. Clin. Microbiol. Antimicrob.*, 2014, 13, 1-6.
- 19 D. Z. Lantzouraki, V. J. Sinanoglou, T. Tsiaka, C. Proestos and P. Zoumpoulakis, *RSC Adv.*, 2015, 5, 101683-101692.
- 20 D. Z. Lantzouraki, V. J. Sinanoglou, P. G. Zoumpoulakis, J. Glamoclija, A. Ciric, M. Sokovic, G. Heropoulos and C. Proestos, *RSC Adv.*, 2015, 5, 2602-2614.
- 21 S. Modaeinama, M. Abasi, M. M. Abbasi and R. J. Esfahlan, *Asian Pac. J. Cancer Prev.*, 2015, 16, 5697-5701.
- 22 M. I. Waly, A. Ali, N. Guizani, A. S. Al-Rawahi, S. A. Farooq and M. S. Rahman, *Asian Pac. J. Cancer Prev.*, 2012, 13, 4051-4055.
- 23 M. N. Aslam, E. P. Lansky and J. Varani, *J. Ethnopharmacol.*, 2006, 103, 311-318.
- 24 M. Dikmen, N. Ozturk and Y. Ozturk, *J. Med. Food*, 2011, 14, 1638-1646.
- 25 P. Panichayupakaranant, A. Itsuriya and A. Sirikatitham, *Pharm. Biol.*, 2010, 48, 201-205.
- 26 U. A. Fischer, R. Carle and D. R. Kammerer, *Food Chem.*, 2011, 127, 807-821.
- 27 F. Wang, D. Scoville, X. C. He, M. M. Mahe, A. Box, J. M. Perry, N. R. Smith, N. Y. Lei, P. S. Davies and M. K. Fuller, *Gastroenterology*, 2013, 145, 383-395.
- 28 G. Holmquist, *Chromosoma*, 1975, 49, 333-356.
- 29 A. Adan, G. Alizada, Y. Kiraz, Y. Baran and A. Nalbant, *Crit. Rev. Biotechnol.*, 2016, 14, 1-14.
- 30 I. Rowe, M. Chiaravalli, V. Mannella, V. Ulisse, G. Quilici, M. Pema, X. W. Song, H. Xu, S. Mari and F. Qian, *Nat. Med.*, 2013, 19, 488-493.
- 31 Q. Zhang, D. Hou, Z. Luo, P. Chen, B. Lv, L. Wu, Y. Ma, Y. Chu, H. Liu and F. Liu, *Cell Death Dis.*, 2015, 6, e1867.
- 32 Y. Zhu, Y. Xia, T. Ye, X. Shi, X. Song, L. Liu, J. Zeng, N. Wang, Y. Luo and Y. Han, *Cell Physiol. Biochem.*, 2014, 33, 933-944.
- 33 K. Garber, *Nat. Biotechnol.*, 2005, 23, 409-411.

- 34 A. J. Hughes, D. P. Spelke, Z. Xu, C. C. Kang, D. V. Schaffer and A. E. Herr, *Nat. Methods*, 2014, 11, 749-755.
- 35 T. Ye, Y. Xiong, Y. Yan, Y. Xia, X. Song and L. Liu, *Plos One*, 2014, 9, e85887.
- 36 E. M. Deqli, *Methods*, 2002, 26, 335-340.
- 37 A. A. Starkov, *Methods Mol Biol.*, 2010, 648, 245-255.
- 38 S. C. Gupta, D. Hevia, S. Patchva, B. Park, W. Koh and B. B. Aggarwal, *Antioxid. Redox Signal.*, 2012, 16, 1295-1322.
- 39 S. O. Yoon, S. J. Park, C. H. Yun and A. S. Chung, *J. Biochem. Mol. Biol.*, 2003, 36, 128-137.
- 40 M. N. Ombra, F. Fratianni, T. Granese, F. Cardinale, A. Cozzolino and F. Nazzaro, *Nat. Prod. Res.*, 2014, 29, 1087-1091.
- 41 H. Park, H. S. Kim, S. J. Eom, K.T. Kim and H.D. Paik, *Molecules*, 2015, 20, 12154-12165.
- 42 H. K. Kwon, J. S. Hwang, J. S. So, C. G. Lee, A. Sahoo, J. H. Ryu, W. K. Jeon, B. S. Ko, C. R. Im and S. H. Lee, *BMC Cancer*, 2010, 10, 392.
- 43 P. Cagle, T. Coburn and P. M. Martin, *AACR*, 2014, 74 (19S).
- 44 T. Ismail, P. Sestili and S. Akhtar, *J. Ethnopharmacol.*, 2012, 143, 397-405.
- 45 L. Wang and M. M. Green, *Int. J. Mol. Sci.*, 2014, 15, 14949-14966.
- 46 L. Sun and X. Wang, *Trends Biochem. Sci.*, 2014, 39, 587-593.
- 47 M. S. Ricci and W. X. Zong, *Oncologist*, 2006, 11, 342-357.
- 48 S. A. Quast, A. C. Berger and J. Eberle. *Cell Death Dis.*, 2013, 4, e839.
- 49 W. Shen, R. Du, J. Li, X. Luo, S. Zhao, A. Chang, W. Zhou, R. Gao, D. Luo, J. Wang, N. Hao, Y. Liu, Y. Chen, Y. Luo, P. Sun, S. Yang, N. Luo and R. Xiang. *Signal Transduct and Targeted Ther*, 2016, 1, 16013.
- 50 J. A. Morrison, L. A. Pike, G. Lund, Q. Zhou, B. E. Kessler, K. T. Bauerle, S. B. Sams, B. R. Haugen and R. E. Schweppe, *Horm. Cancer*, 2015, 6, 87-99.
- 51 Y. L. Jia, L. Shi, J. N. Zhou, C. J. Fu, L. Chen, H. F. Yuan, Y. F. Wang, X. L. Yan, Y. C. Xu and Q. Zeng, *Hepatology*, 2011, 54, 1808-1818.
- 52 E. J. Lee, S. J. Lee, S. Kim, S. C. Cho, Y. H. Choi, W. J. Kim and S. K. Moon, *Cell Signal.*, 2013, 25, 2025-2038.

Table and Figure Legends

Fig.1. HPLC and MS. (A) Chromatogram of PoPx, PC (peak 1 and peak 2) and EA (peak 3). (B) The chemical structure of PC and EA. (C) The molecular weight of EA (ellagic acid [M-H]⁻: 301.3) and PC (punicalagin [M-H]⁻: 1083.2).

Fig.2. Inhibition of cell growth and colony formation on human cancer cell lines BCPAP and TPC-1 by PoPx. (A) Cells were exposed to various doses of PoPx (0-200µg/mL) for 48h and cell morphologic changes were assessed (×10). (B) Proliferation of BCPAP, TPC-1 and Nthy-ori 3-1 cells treated with various concentrations (0-200µg/mL) of PoPx for 24, 48 and 72h, respectively. Cell viability was evaluated by MTT assay. Data are expressed as means ± SD from three experiments (**p*<0.05; ***p*<0.01; ****p*<0.001 vs. vehicle control). (C) The effect of PoPx (0-200µg/mL) on colony formation in BCPAP and TPC-1 cell lines for 10 days, the statistic results of colony formation assays presented as surviving colonies. Data are expressed as means ± SD from three experiments (**p*<0.05; ***p*<0.01; ****p*<0.001 vs. vehicle control).

Fig.3. PoPx induces thyroid cancer cells apoptosis. (A) Cell nuclear changes of BCPAP and TPC-1 cells were determined by staining with Hoechst 33258 and visualized by fluorescence microscope after treatment with increasing doses of PoPx for 48h (×40). (B) BCPAP and TPC-1 cells were treated with PoPx at indicated doses for 48h, and the level of apoptosis was evaluated using the Annexin V/PI dual-labeling technique, and determined by FCM. (C) The proportions of apoptotic cells, including the early apoptotic cells (LR, positive for Annexin V only) and the late apoptotic cells (UR, Annexin V and PI-positive), were analysed after various concentrations (0-200µg/mL) of PoPx treatment for 48h. Data are expressed as means ± SD from three experiments (**p*<0.05; ***p*<0.01; ****p*<0.001 vs. vehicle control). (D) Western blot analyses of BCPAP cells treated (48h) with different concentrations (0, 25, 100 and 200µg/mL) of PoPx were to evaluate protein expression of Bax and MMP-9. Protein expression was quantified by the densitometry analysis using Image J and normalized against β-actin expression. Statistic of the relative expression of Bax increased and MMP-9 decreased after treatment with PoPx was shown on the right. Data are expressed as means ± SD from three experiments (**p*<0.05; ***p*<0.01; ****p*<0.001 vs. vehicle control).

Fig.4. Effects of PoPx via the intrinsic apoptosis pathway. (A, B and C) PoPx reduced the mitochondrial membrane potential ($\Delta\Psi_m$) in BCPAP and TPC-1 cells. BCPAP and TPC-1 cells were treated with various concentrations (0-200 $\mu\text{g}/\text{mL}$) of PoPx for 48h and then stained with 10 μM Rh123 to detect the change of $\Delta\Psi_m$ by FCM. Data are expressed as means \pm SD from three experiments (* p <0.05; ** p <0.01; *** p <0.001 vs. vehicle control). BCPAP (D) and TPC-1 (E) cells were treated with designed concentrations (0-200 $\mu\text{g}/\text{mL}$) of PoPx for 48h. The harvested cells were loaded with 10 μM DCFH-DA and then ROS levels in cells were measured by FCM. (F) Quantification of ROS is shown. Data are expressed as means \pm SD from three experiments (* p <0.05; ** p <0.01; *** p <0.001 vs. vehicle control).

Fig.5. PoPx inhibits thyroid cancer cells BCPAP and TPC-1 migration and invasion. (A) PoPx inhibits BCPAP and TPC-1 migration. Tumor cells were seeded in the top chamber of transwell with serum-free medium and treated with vehicle or designed concentrations (25, 100, 200 $\mu\text{g}/\text{mL}$) of PoPx. After about 48h, migrated cells were fixed, stained, photographed ($\times 20$) and quantified (* P <0.05, ** P <0.01, *** P <0.001). (B) PoPx inhibits BCPAP and TPC-1 invasion. Tumor cells were planted in which were pre-treated with Matrigel on the upper chamber membrane and treated with various concentrations (0, 25, 100, 200 $\mu\text{g}/\text{mL}$) of PoPx, and the bottom chamber was filled with the complete medium containing 10% FBS. After about 48h, invaded cells were fixed, stained, photographed ($\times 20$) and counted. (* P <0.05, ** P <0.01, *** P <0.001).

Fig.6. Antitumor effects of PoPx *in vivo*. (A) Tumors were visualized to show the inhibitory effect of PoPx on BCPAP tumor 24 days after subcutaneous ectopic cell implantation. (B) Representing weight of tumor from mice of different groups, respectively. Data are expressed as means \pm SD (n=5; ** P <0.01). (C) Tumor size was measured and calculated every three days and presented as means \pm SD (n=5; * P <0.05, ** P <0.01, *** P <0.001). (D) The difference of body weight between two administrated groups and one vehicle group were not significant. Data are expressed as means \pm SD. (E, F and G) Tumors were fixed in formalin, processed for paraffin embedding and then stained with CC-3, Ki-67 and MMP-9 using the DAB Detection Kit. Images shown are representatives from each group ($\times 20$). (E) Apoptosis was

measured on paraffin-embedded BCPAP tumor sections by CC-3 immunohistochemical staining. The statistical data of CC-3 positive cell number were shown on the right. (F) Tumor cell proliferation was evaluated through immunohistochemical analysis staining with Ki-67, and the statistical data of Ki-67 positive cell number were shown on the right. (G) Immunohistochemistry was performed to measure the expression of MMP-9 in tumor tissues isolated from vehicle and PoPx-treated mice. The treatment with PoPx reduced MMP-9-positive cells versus vehicle group. (* $P < 0.05$; ** $P < 0.01$ vs. vehicle control)

Fig.7. Evaluation of the damage of PoPx to visceral organs of animals. Mice were divided into 3 groups and intragastric administration (i.g.) with PoPx 125mg/kg, 62.5mg/kg or vehicle. After 31 days, animals were sacrificed and the main organs were obtained for further study. H&E staining of paraffin-embedded sections of heart, liver, spleen, lung and kidney are shown from BCPAP tumor-bearing mice. ($\times 20$)

Table 1

Linear range, regression equation and R^2 of EA and PC.

Component	Linear range (mg/L)	Regression equation	R^2
EA	50-500	$^a y = 149530x + 2 \times 10^6$	0.9935
PC	125-2000	$^a y = 2 \times 10^7 x - 6 \times 10^6$	0.971

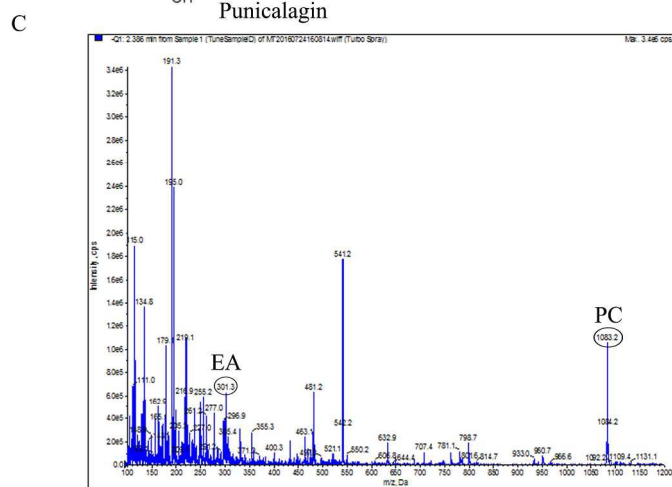
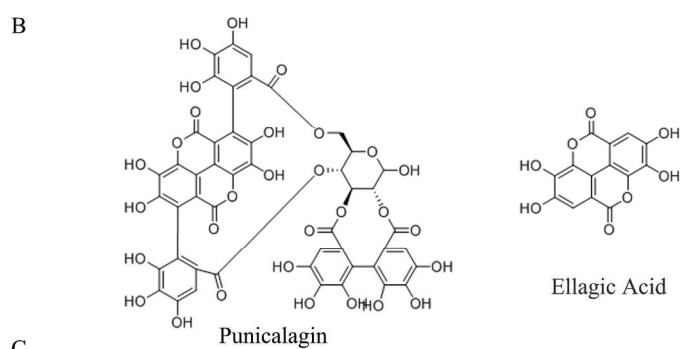
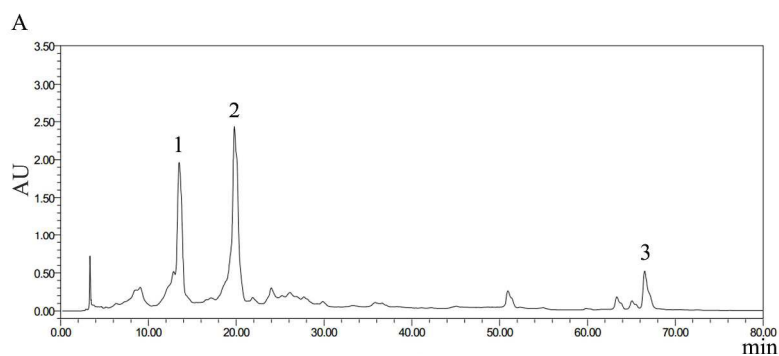
$^a y$ is the peak area; x refers to the concentration of compound (mg/L).

Table 2

The effect of PoPx on normal cell lines viability.

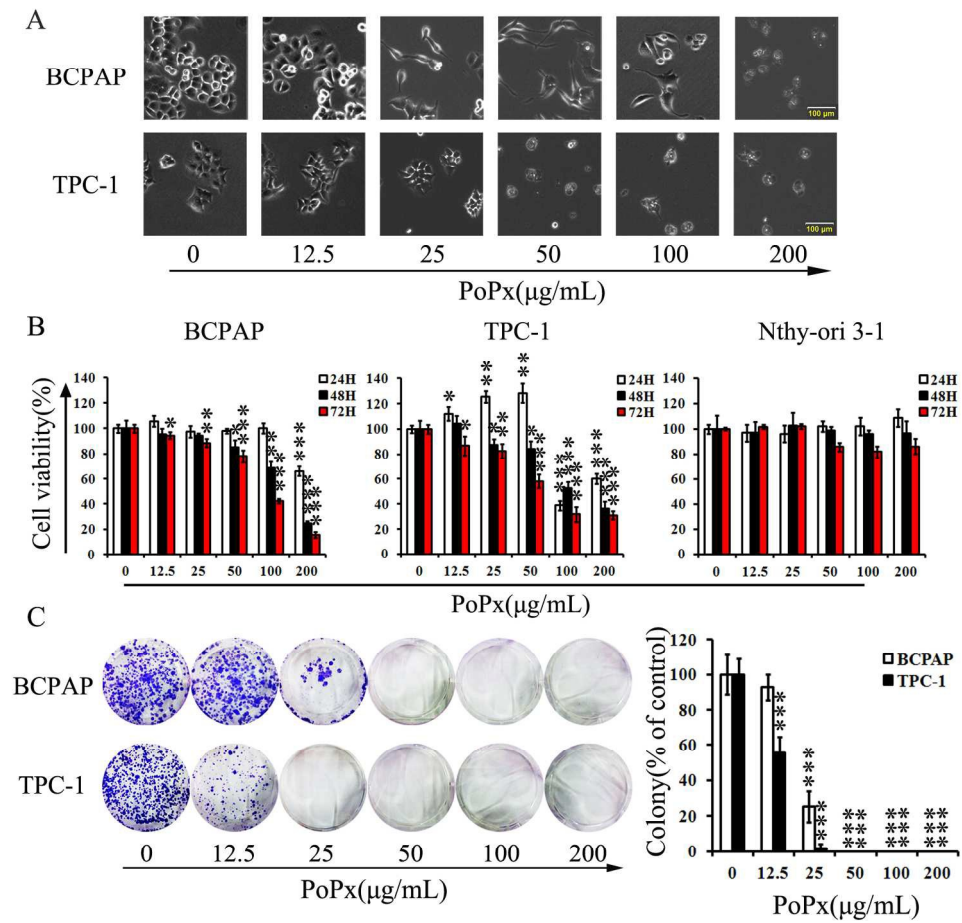
Cell lines	Cell type	IC50 ($\mu\text{g/mL}$)
Nthy-ori 3-1	Human thyroid follicular epithelial cell line	>400
HEK293	Human embryonic kidney cell line	>400
LO2	Human normal liver cell line	>400

Each cell line was treated with various concentrations (0, 12.5, 25, 50, 100, 200 $\mu\text{g/mL}$) of PoPx for 72h. MTT assay was used to determine the IC50 values. Data are expressed as means \pm SD for three independent experiments.



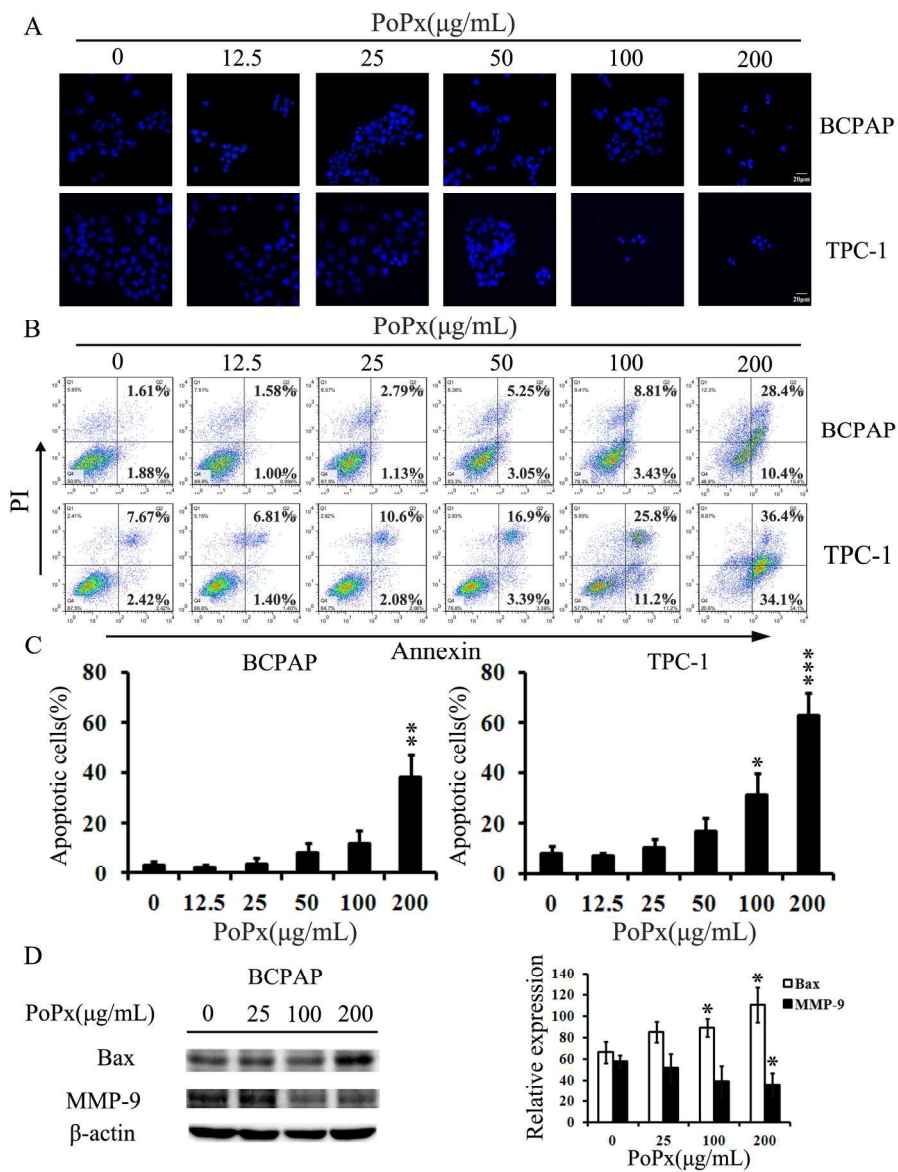
HPLC and MS

231x335mm (300 x 300 DPI)



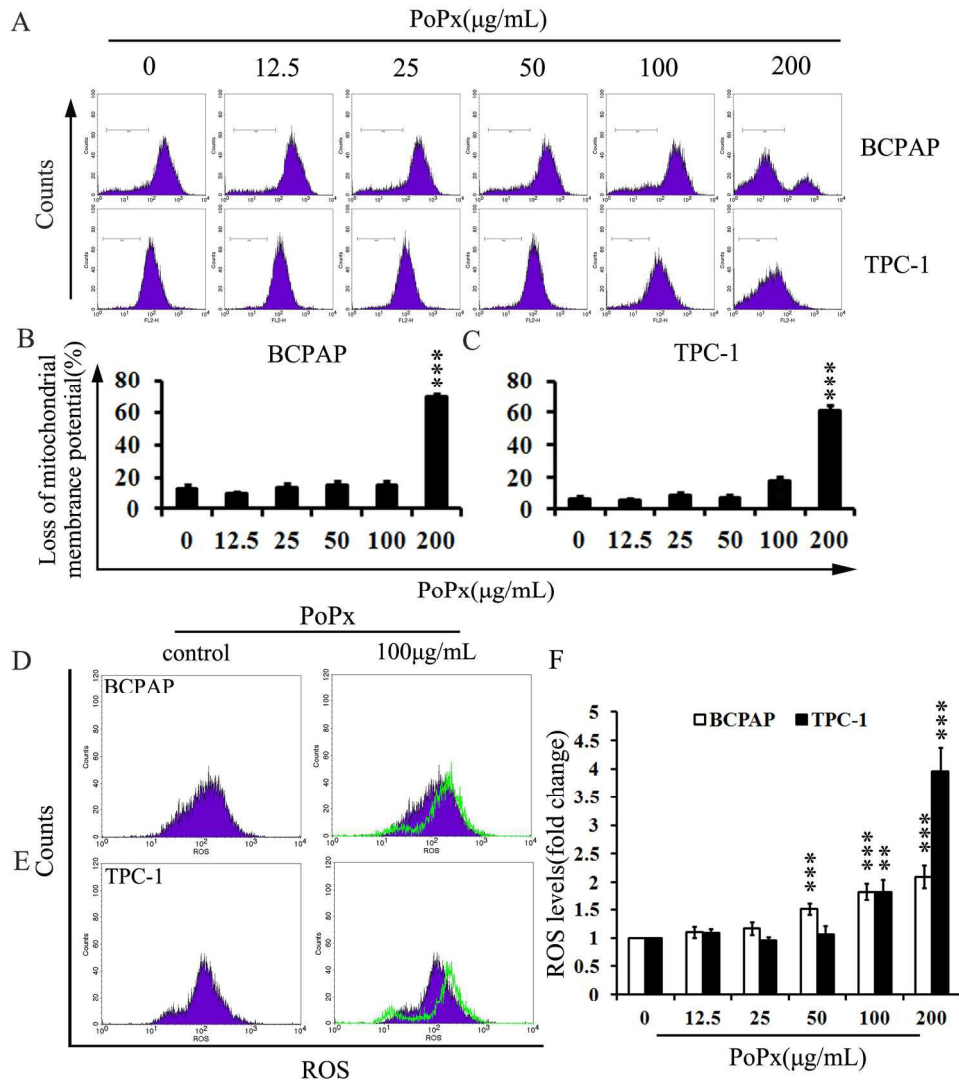
Inhibition of cell growth and colony formation on human cancer cell lines BCPAP and TPC-1 by PoPx.

175x170mm (300 x 300 DPI)



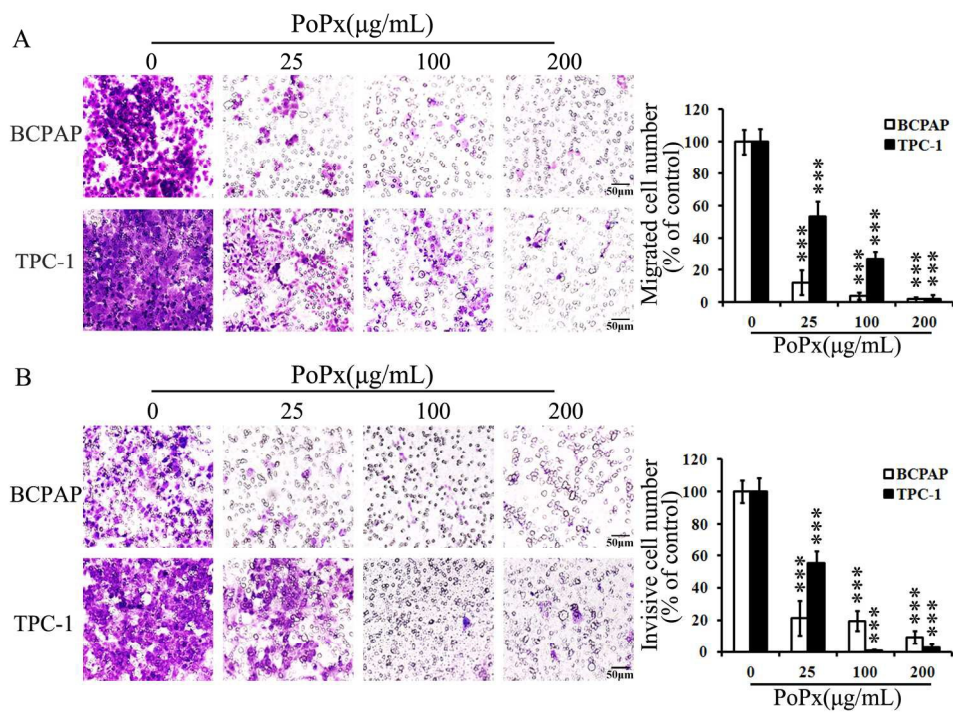
PoPx induces thyroid cancer cells apoptosis.

175x224mm (300 x 300 DPI)



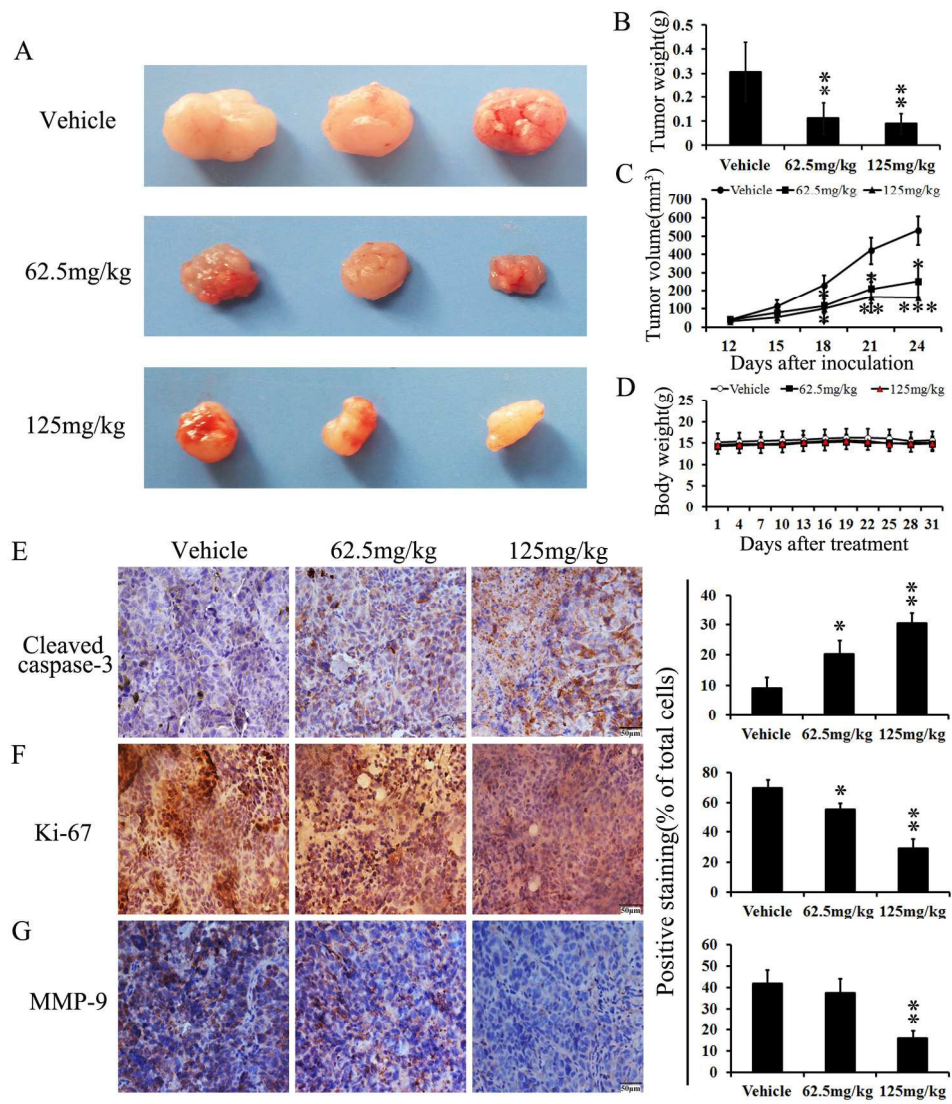
Effects of PoPx via the intrinsic apoptosis pathway.

177x199mm (300 x 300 DPI)



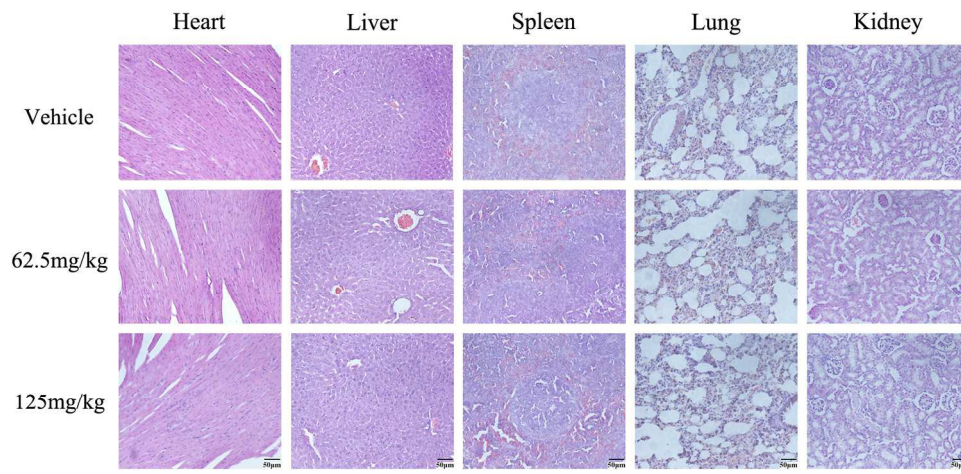
PoPx inhibits thyroid cancer cells BCPAP and TPC-1 migration and invasion.

189x144mm (300 x 300 DPI)



Antitumor effects of PoPx in vivo.

180x204mm (300 x 300 DPI)



Evaluation of the damage of PoPx to visceral organs of animals.

170x87mm (300 x 300 DPI)